The effect of Zn metallophthalocyanine on the optical and structural properties of sol-gel spin coated TiO$_2$ thin films

HASAN SARIGÜL[a], İBRAHİM ÖZÇEŞMECİ[b], İDRİS SORAR[a,*]
aDepartment of Physics, Hatay Mustafa Kemal University, TR-31060, Antakya, Hatay, Turkey
bDepartment of Chemistry, Istanbul Technical University, TR-34469, Maslak, Istanbul, Turkey

In this study, TiO$_2$, TiO$_2$/ZnPc and ZnPc thin films were deposited on glass substrates by spin coating method and the effect of ZnPc doping concentration on the optical and structural properties of the films was investigated. A spectrophotometer in the 300-1100 nm wavelength range was used to measure the optical transmittance of thin films. UV-Vis studies showed that transmittance of the films decreased with the increasing concentration of ZnPc in the ranges corresponding to the B and Q band absorption regions, which are the characteristic peaks of phthalocyanines between 300–400 nm and 600–700 nm, respectively. Scanning electron microscopy (SEM) was used to characterize the surface morphology of thin films and they were observed to be homogeneously coated. X-ray measurements of annealed films showed an anatase-brookite mixed phase and it was found that crystal size decreased with increasing ZnPc concentration.

1. Introduction

In the production of advanced technological devices, materials with certain optical and electrical properties are needed. New materials with these properties not only deeply affect existing products, but also enable the development of new technologies. Organic semiconductor thin films have various electrical and optical properties. They can be used in sophisticated technological devices [1], such as sensors [2], organic light emitting diodes (OLED) [3, 4], organic field effect transistors (OFETs) [5], and organic photovoltaics (OPVs) [6].

Among organic materials, phthalocyanines (Pc) are highly delocalized 18-π electron synthetic compounds showing powerful absorption in the visible region corresponding to the π-π* transition. Hence, they exhibit number of particular optical, structural, and electronic properties which make them of major interest in various application areas ranging from nanotechnology to medicine such as electrochromic display devices [7], catalysis [8], non-linear optics [9], photodynamic therapy [10], optical data storage [11], chemical sensors [12], liquid crystals [13], semiconductor devices [14], dye-sensitized solar cells [15] and Langmuir-Blodgett films [16]. However, poor solubility is the biggest factor preventing widespread usage of Pcs. Encouraging way to solve this solubility problem of Pcs is to alter their peripheral ring by introducing certain substituent [17]. Among the depositions methods of Pcs films, vacuum and Langmuir-Blodgett are the most common methods. However, the spin coating technique, which enables the production of useful and a practical device, is one of the easiest and the most convenient method for obtaining thin films [18]. With this method, the thickness and optical properties of the film can be easily modified with the starting solution (concentration, solid ratio, drying speed and surface tension) and/or the coating process condition such as rotation time, and rotation speed [19].

Titanium dioxide (TiO$_2$) is considered as one of the most promising semiconductor material with its unique electrical and optical properties [20]. Furthermore, TiO$_2$ is widely used with the increasing interest in many fields and applications due to its cheapness, nontoxicity, resistance to corrosion and excellent chemical stability [21–24]. There are several promising uses of TiO$_2$ films such as hydrogen production [25], water purification [24], gas sensor [26], solar cells devices [27], optoelectronic devices [28], and so on. Besides the amorphous structure, TiO$_2$ is also available in three crystalline phases: anatase, brookite and rutile forms.

There are many important reasons to study the optical properties of materials with a wide range of wavelengths used in optical applications, such as optical filters, optical gas sensors, solar cells and reflective coatings, and it is necessary to have accurate information about them. Therefore, in this study, we investigated the optical properties of combination of ZnPc functionalized with peripheral bulky 9-anthroyl substituents through flexible oxyethylthio-bridges and TiO$_2$ films. Electronic absorption spectra of zinc (II) phthalocyanine containing bulky group (anthracene) was studied in different organic solvents. Scanning electron microscopy (SEM) was used to characterize the surface morphology of the films. Some information about optical properties of the films such as transmittance and absorption were recorded using UV-Vis spectrometer.

2. Experimental procedure

2.1. The effect of solvent on the electronic absorption spectra

Tetrakis(9-anthroylethylthio)zinc(II)phthalocyanine (ZnPc) was synthesized according to the reported procedures (Scheme 1) [29].
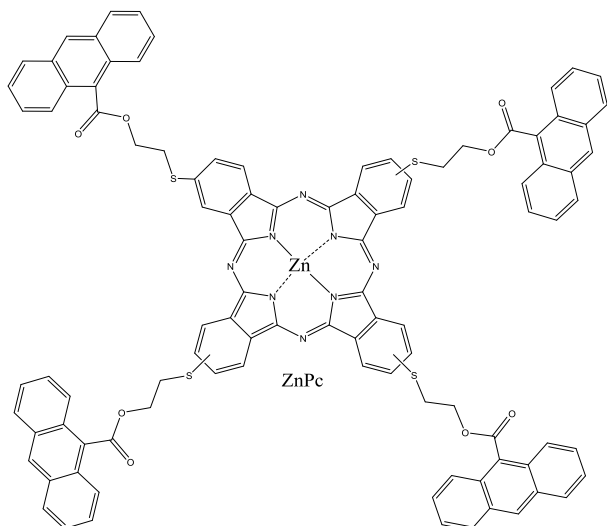
Scheme 1. The structure of ZnPc

In this part of the study, the electronic absorption spectra of zinc (II) phthalocyanine containing bulky group (anthracene) in different organic solvents were also analyzed (Fig. 1).
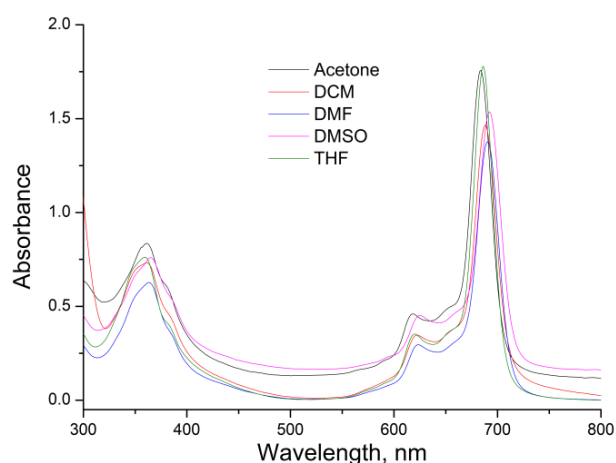
Fig. 1. Electronic absorption spectra of ZnPc in different solvents (color online)

Normally, phthalocyanine compounds have typical electronic spectra with two strong absorption regions. The first of them is B band (around 300–400 nm) caused by deeper π levels in the UV region → the lowest unoccupied molecular orbital (LUMO) transition. The other is Q band (around 600–700 nm) attributed to the π–π* transition from the highest occupied molecular orbital (HOMO) to the

LUMO of the Pcs^{-2} ring [30, 31]. The characteristic Q band transition of metallo phthalocyanine with D_{4h} symmetry is observed as a single band of high intensity [32].

It is known that the position of the Q-band varies by solvent [33]. In this study, Q band was observed as expected single peak at 692 nm in dimethyl sulfoxide (DMSO), 690 nm in dimethylformamide (DMF), 688 nm in dichloromethane (DCM), 686 nm in tetrahydrofuran (THF) and 684 nm in acetone. While the shortest wavelength was observed in acetone, the longest Q-band wavelength was observed in DMSO. This result can be explained by considering the refractive indices of the solvents. It has been observed that the values of the Q band absorption spectra vary according to the solvents. These results are function of the refractive index of the solvent originally described by Bayliss [34, 35]. Fig. 2 display a plot of the Q-band frequency *vs.* the function $(n^2 - 1)/(2n^2 + 1)$, where n is the refractive index of the solvent. The change of Q band values in solvers shows a linear dependence as can be seen in Fig. 2. This result shows that the shifts are mostly due to solvation and not the ligation effect [34].
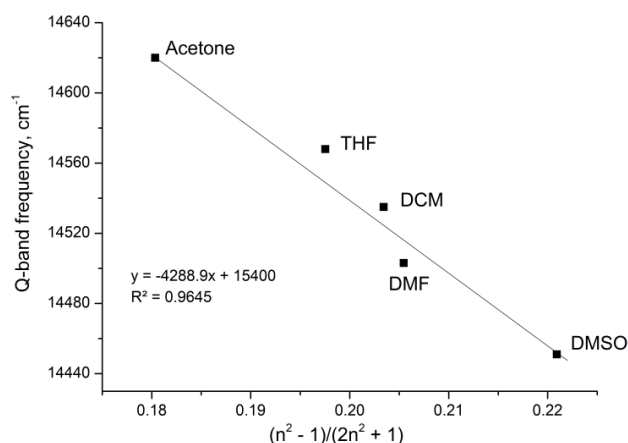
Fig. 2. Plot of the Q-band frequency of ZnPc against $(n^2 - 1)/(2n^2 + 1)$, where n is the refractive index of the solvent

2.2. Preparation of thin film

Titanium oxide solution was prepared using the precursors of titanium (IV) butoxide [$Ti(OCH_2CH_2CH_2CH_3)_4$, 97%, Sigma-Aldrich], absolute ethyl alcohol (CH_3CH_2OH) and glacial acetic acid (CH_3COOH). Ethyl alcohol and acetic acid were first mixed together for 10 min through a magnetic stirrer. Then, titanium butoxide was added slowly to this solvent and stirred for 1 h at room temperature. Final solution was transparent, clear, and stable. ZnPc solution was prepared by dissolving ZnPc in dimethylformamide [$(CH_3)_2NC(O)H$] with different concentrations. DMF is well-known as a dispersing agent [36]. Then these two solutions, ZnPc and TiO_2, were mixed at room temperature and stirred for 1 hour in different ratios of TiO_2/ZnPc(x) where $x = 0.5$–4.0 mg as summarized in Table 1.

The microscope glass substrates were cleaned with 1/5 diluted sulfuric acid, ethanol and deionized water by using

an ultrasonic bath and finally dried on a hot plate. After the solutions were dropped onto the substrates, they were spun at 2000 rpm for 30 seconds. Then films were dried at 100 ºC for 5 minutes on a hot plate. The coating/drying process was repeated for 5 times, except ZnPc film which was coated as mono-layer. The name of each film was labeled with the name of the solvent from which it was prepared.

Table 1. Attributions of solutions and their ratios used in the preparation of TiO₂/ZnPc thin films.

Solution designation	TiO₂ solution(ml)	ZnPc solution(mg)	DMF(µl)
TiO₂	5	-	-
TiO₂/ZnPc(0.5)	5	0.5	100
TiO₂/ZnPc(1.0)	5	1	100
TiO₂/ZnPc(2.0)	5	2	100
TiO₂/ZnPc(3.0)	5	3	100
TiO₂/ZnPc(4.0)	5	4	100
ZnPc	-	4	100

The crystal structure of the coated films was determined by X-ray diffraction (XRD) using a Rigaku Smart Lab diffractometer with CuKα radiation (λ = 0.154059 nm). The microstructure of coated films was examined with SEM. The optical investigation of the films was performed by using a Thermo Scientific GENESYS 10S UV–vis spectrophotometer in the wavelength range of 300–1100 nm.

3. Results and discussion

3.1. Structural analysis

Pure TiO₂ films that are not annealed or annealed below about 500 °C are known to be amorphous [37]. Hence, the samples have been annealed at 550 °C for 90 minutes to achieve a crystalline film structure. Annealed TiO₂ and ZnPc doped TiO₂ films were examined with XRD spectra as shown in Fig. 3 to determine the phase and crystal structure of thin films. All peaks of the anatase structure, except for one brookite structure, were observed. Mixed phase has been previously seen in a similar study [38]. The XRD spectra show no impurity peaks. The peak planes of the films (101), (004), (112), (200), (105), and (211) correspond to anatase structure by International Center for Diffraction Data (ICDD) card number 01-075-2547 and (121) correspond to brookite structure by ICDD card number 00-029-1360. Most sharp diffraction peak appeared at range $2\theta = 25.32^{o}$ for pure TiO₂ and 25.23^{o} for ZnPc doped TiO₂ films. It can be seen that the peaks slightly shift towards lower 2θ values with increasing the ZnPc content in Fig. 3a. The most intense atomic peaks of TiO₂, TiO₂/ZnPc(0.5) and TiO₂/ZnPc(2.0) samples are plotted in Fig. 3b and the peak shifts can be clearly seen from this figure. This shift can be explained by the fact that an increase in the TiO₂/ZnPc(x) unit cell will cause the 2θ diffraction angles to move towards lower angles due to Bragg's law. The peak intensity decreased with the increase of ZnPc amount and an amorphous structure was observed for TiO₂/ZnPc(4.0) film. The more ZnPc doping to the TiO₂ lattice prevents further growth of the crystal structure.
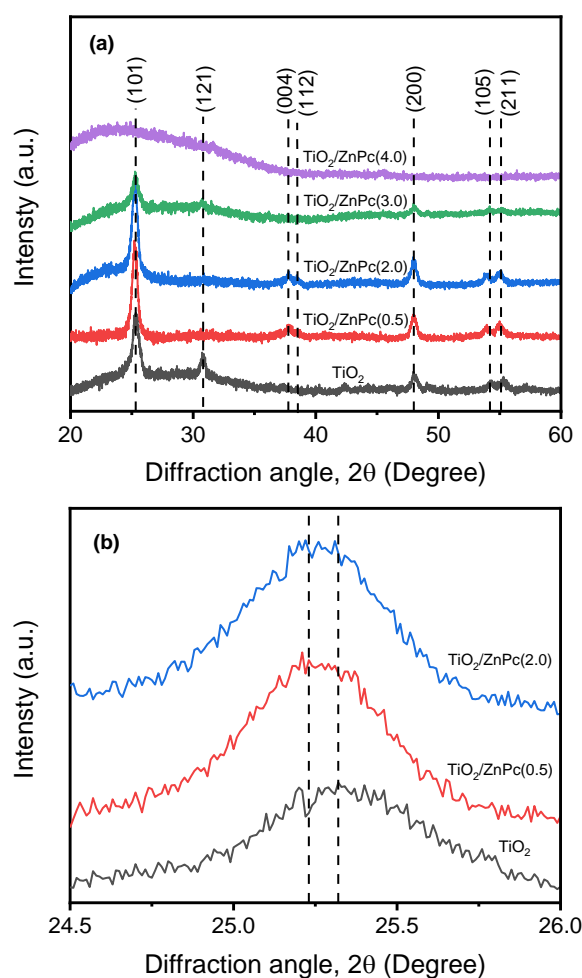

Fig. 3. a) XRD pattern of TiO₂ and ZnPc doped TiO₂ thin films. The peaks are assigned to the shown atomic planes; b) The peak shift representing the atomic plane of (101) (color online)

Scherrer formula was used to determine the crystallite size (D) of the anatase structure [39]:

$$D = \frac{K\lambda}{\beta Cos\theta} \tag{1}$$

where β is the broadening of diffraction line measured at half of its maximum intensity in radians FWHM, λ is wavelength of X-ray (1.5406 Å), and θ is the angle of (101) plane. The calculated average size of crystallites for (101) of bare TiO_2 and ZnPc doped TiO_2 films are presented in Table 2 and plotted in Fig. 4. The calculated values of the crystallite size ranged from 18.09 nm to 11.80 nm. The

ZnPc molecules may not have easily incorporate the TiO_2 lattice because it is larger molecule structure than titania. ZnPc molecules may also be evaporated during the annealing process. Brookite plane (121) and anatase (004), (112), (105), and (211) planes disappeared in TiO_2/ZnPc (3.0) films.

Table 2. Structural properties of annealed TiO_2 and ZnPc doped TiO_2 thin films

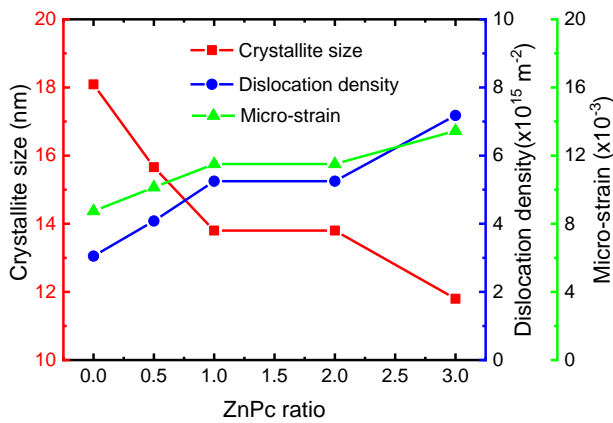| Thin film	2θ (degree)	FWHM	D (nm)	δx10^15 (m^-2)	εx(10^-3)	d-spacing (Å)
TiO_2	25.32	0.45	18.09	3.05	8.74	3.51
TiO_2/ZnPc(0.5)	25.23	0.52	15.66	4.08	10.14	3.53
TiO_2/ZnPc(1.0)	25.23	0.59	13.80	5.25	11.50	3.53
TiO_2/ZnPc(2.0)	25.23	0.59	13.80	5.25	11.50	3.53
TiO_2/ZnPc(3.0)	25.23	0.69	11.80	7.18	13.45	3.53

Fig. 4. Comparison of crystallite size, dislocation density and micro-strain for bare TiO_2 and TiO_2/ZnPc(x) (x = 0.5, 1.0, 2.0 and 3.0) films (color online)

A unit cell is smallest block in crystal lattice. This periodicity of unit cell in 3D space made crystal structure. However, imperfections and dislocations in the material spoil the crystal structure. The dislocation density (δ) is determined from the formula [40]:

$$\delta = 1/D^2 \qquad (2)$$

Dislocation density increases with increasing amount of ZnPc, which indicates that crystal defects increase. There are three mechanisms that cause dislocations: nucleation, interface between lattice and surface, and grain boundary formation. The shift of a dislocation is obstructed by distinct dislocations in thin films. Therefore, the smaller crystallite size is caused by the greater dislocation density. On the other hand, increasing dislocation density causes greater hardness. It shows that higher amount of ZnPc doped TiO_2

are stronger and harder than other annealed crystalline TiO_2 films with less doping. It is known that the strength of materials increases with further decrease in crystallite size below~20 nm [38].

Micro-strain (ε) caused by crystal defects was calculated according to Ref. [41]:

$$\varepsilon = \beta/4\tan\theta \qquad (3)$$

There is an insignificant increase in strain with higher ZnPc doping rates. The peaks become wider as the crystallite size decreases. This is the result of micro strains resulting from dislocation and twinning within the crystal structure. When the ZnPc content increased, the strain increased. This growth is due to the recrystallization of polycrystalline thin films on the substrate [38].

3.2. Morphological and optical analysis

High-resolution SEM images of TiO_2 and TiO_2/ZnPc(x) films are illustrated in Fig. 5. These images showed that the films have surface morphologies with uniformly distributed nano-sized pores which surround the clustered TiO_2 particles. It can be seen that these pores narrowed and decreased as the ZnPc amount of the film is increased. This is an evident that ZnPc addition to the film modifies the surface morphology. At the same time, it is seen that these clustered particles are also getting smaller. This trend in the SEM surface morphology is also consistent with the XRD result that the addition of ZnPc to TiO_2 films reduces the crystallite size as seen in Table 2. On the other hand, ZnPc films have been observed to form a more continuous and particulate-free structure compared to TiO_2 and TiO_2/ZnPc(x). The average thickness of the films was determined from SEM cross-section and found to be about ~400–450 nm.
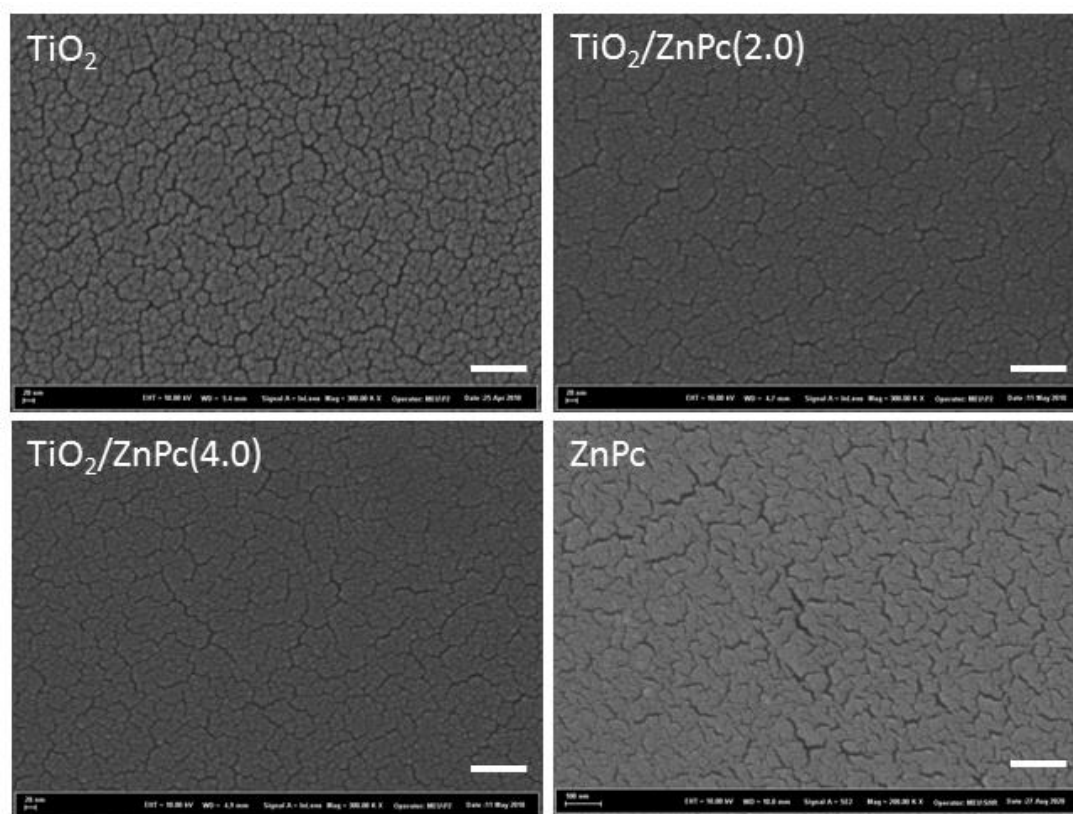
Fig. 5. Scanning electron microscopy images of for bare TiO₂, ZnPc doped TiO₂ and bare ZnPc films. Sample designations are stated. Magnification of TiO₂ and ZnPc doped TiO₂ films are 300 kX and 200 kX for ZnPc, respectively. The scale bars for TiO₂ and TiO₂/ZnPc(x) are 100 nm, and it is 150 nm for ZnPc

Optical analysis of thin films is very beneficial in showing the energy gap and band structure of both crystalline and amorphous structures [42]. The optical transmittance spectra and absorbance spectra in the range between 300 nm and 1100 nm were presented in Fig. 6 and Fig. 7, respectively. As seen in the figures, the non-annealed TiO₂, TiO₂/ZnPc and ZnPc thin film has good transmittance in the visible range. The optical transmission spectra of TiO₂ films showed high transmittance more than other ZnPc doped TiO₂ films in most of the spectrum.
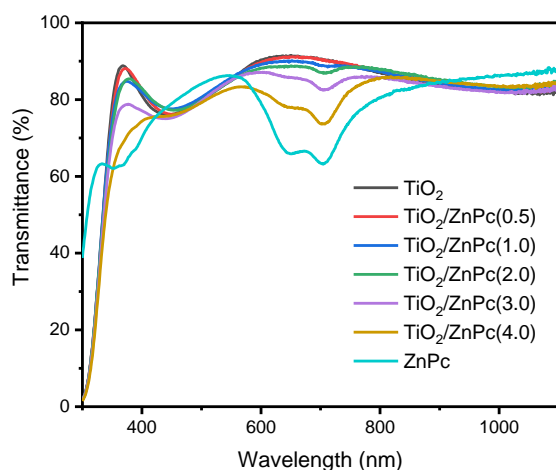

Fig. 6. Spectral transmittance for bare TiO₂, ZnPc doped TiO₂ and bare ZnPc films deposited onto glass substrate (color online)
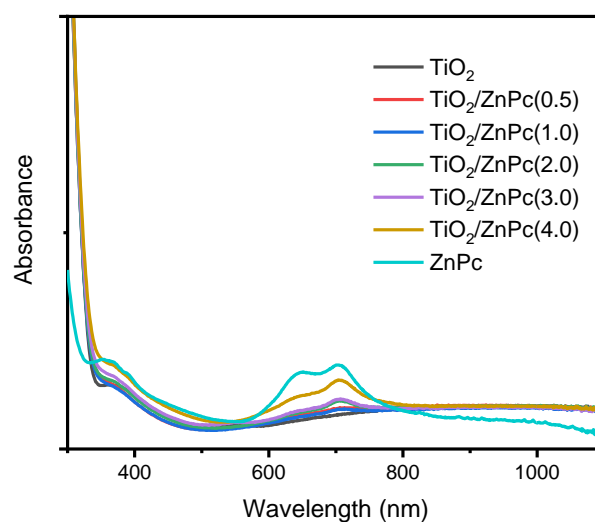

Fig. 7. Absorbance spectra for bare TiO₂, ZnPc doped TiO₂ and bare ZnPc films deposited onto glass substrate (color online)

High absorption was observed in wavelengths below the ~350 nm for all of the samples. The peak of transmittance drop from %89 to %63 with increase of ZnPc amount at about 367 nm. Above the wavelength of 800 nm, all the films have high transparency with an approximate value of 82–87%. The band, which is around 350 nm, is caused by electronic transitions between molecules of moderate ionic grade that match the synthesized molecular

materials. Phthalocyanine thin films absorb light on both sides of the blue-green region and can be used as photoconductors [1]. The Q band absorption of TiO_2/ZnPc and pure ZnPc films was showed peak about 700 nm. Also, TiO_2/ZnPc(3.0), TiO_2/ZnPc(4.0) and ZnPc films showed secondary peak at about 645 nm. The minimum transmittance rate of the films in the Q band region are 90%, 89%, 87%, 82%, 74%, 63% at around 700 nm for TiO_2/ZnPc(0.5), TiO_2/ZnPc(1.0), TiO_2/ZnPc(2.0), TiO_2/ZnPc(3.0), TiO_2/ZnPc(4.0) and ZnPc films, respectively. The results showed that the different amount of ZnPc in the starting solution prepared to coat the films clearly change the transmittance rate minimum in Q band region of TiO_2/ZnPc films. The decrease in transmittance in general, and especially in the Q band region, as the amount of ZnPc of the film increases is also evident from the decrease of pores in the SEM surface morphology in Fig. 5.

The optical band gap energy of the MPc films was evaluated making use of the equation described in [43], and the graph of the photon energy vs. $(\alpha h\nu)^2$ is shown in Fig. 8. The results show that band gap energy values of TiO_2 and TiO_2/ZnPc thin films were changed in the range of 4.05–4.09 eV. The band gap energy value of bare ZnPc thin film was 4.54 eV. It can be seen that the ZnPc ratio of TiO_2/ZnPc(x) films—prepared by doping zinc (II) phthalocyanine containing bulky group (anthracene) to the starting solution—significantly changes their band gap energies.
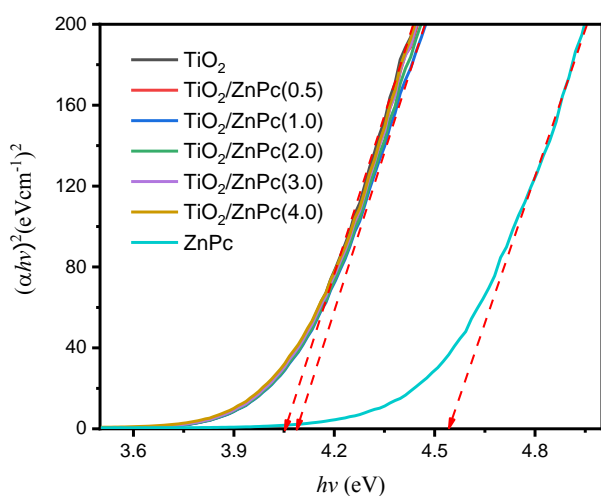

Fig. 8. Relation between $(\alpha h\nu)^2$ vs. photon energy for bare TiO_2, ZnPc doped TiO_2 and bare ZnPc films deposited onto glass substrate (color online)

4. Conclusion

In summary, thin films of TiO_2, TiO_2/ZnPc and ZnPc were successfully deposited onto the glass substrate using sol-gel spin coating method. The SEM images of the films showed that TiO_2 and TiO_2/ZnPc were homogenously coated with uniformly distributed nano-sized pores which surround the clustered TiO_2 particles and ZnPc films had continuous and particulate-free structure. The optical measurements of TiO_2/ZnPc thin films showed that

transmittance values minima around Q band region were changed significantly in respect to amount of ZnPc. The energy band gaps of TiO_2/ZnPc thin films were approximately in the range of 4.05–4.09 eV and pure ZnPc film's value was 4.54 eV. These results show that the novel TiO_2/ZnPc films have specific features desirable for optoelectronic devices.

References

[1] S. Pourteimoor, M. E. Azim-Araghi, Mater. Sci. Semicond. Process. **18**, 97 (2014).
[2] A. N. Sokolov, M. E. Roberts, Z. Bao, Mater. Today **12**(9), 12 (2009).
[3] C. Zhang, P. Chen, W. Hu, Small, **12**(10), 1252 (2016).
[4] J. Lee et al., Nat. Mater. **15**(1), 92 (2016).
[5] S. Vegiraju et al., Adv. Funct. Mater. **27**(21) 1606761 (2017).
[6] P. Cheng, G. Li, X. Zhan, Y. Yang, Nat. Photonics **12**(3), 131 (2018).
[7] G. de la Torre, M. Nicolau, T. Torres, Supramol. Photosensit. Electroact. Mater., Elsevier, 1 (2001).
[8] A. B. Sorokin, Chem. Rev. **113**(10), 8152 (2013).
[9] M. M. Ayhan et al., Inorg. Chem. **53**(9), 4359 (2014).
[10] X. Li et al., Coord. Chem. Rev. **379**, 147 (2019).
[11] M. Hanack, M. Lang, Adv. Mater. **6**(11), 819 (1994).
[12] M. Pişkin, N. Can, Z. Odabaş, A. Altındal, J. Porphyr. Phthalocyanines **22**(01n03), 189 (2018).
[13] M. Yatabe, A. Kajitani, M. Yasutake, K. Ohta, J. Porphyr. Phthalocyanines **22** (01n03), 32 (2018).
[14] R. Ghanem, Spectrochim. Acta. A. Mol. Biomol. Spectrosc. **72**(3), 455 (2009).
[15] L. Giribabu et al., Dyes Pigments **98**(3), 518 (2013).
[16] L. Valli, Adv. Colloid Interface Sci., **116**(1-3), 13 (2005).
[17] I. Özçesmeci, S. Güner, A. I. Okur, A. Gül, J. Porphyr. Phthalocyanines **11**(07), 531 (2007).
[18] İ. Sorar, İ. Özçeşmeci, A. Gül, Prot. Met. Phys. Chem. Surf. **55**(5), 1019 (2019).
[19] İ. Özçeşmeci, I. Sorar, A. Gül, Inorg. Chem. Commun. **14**(8), 1254 (2011).
[20] D. K. Muthee, B. F. Dejene, Mater. Sci. Semicond. Process **106**, 104783 (2020).
[21] J. Du et al., ACS Nano **5**(1), 590 (2011).
[22] C. H. Kwon, H. Shin, J. H. Kim, W. S. Choi, K. H. Yoon, Mater. Chem. Phys. **86**(1), 78 (2004).
[23] S. Nezar et al., Appl. Surf. Sci. **395**, 172 (2017).
[24] A. Wold, Chem. Mater. **5**, 280 (1993).
[25] A. Fujishima, X. Zhang, D. Tryk, Surf. Sci. Rep. **63**(12), 515 (2008).
[26] K. Zakrzewska, Thin Solid Films **391**(2), 229 (2001).

[27] W. R. Duncan, O. V. Prezhdo, Annu. Rev. Phys. Chem. **58**(1) 143 (2007).

[28] K. Kalyanasundaram, Coord. Chem. Rev. **177**(1), 347 (1998).

[29] İ. Özçeşmeci, O. Güney, A. İ. Okur, A. Gül, J. Porphyr. Phthalocyanines **13**(06) 753 (2009).

[30] M. Özçeşmeci, S. Sancar-Baş, B. Akkurt, E. Hamuryudan, Ş. Bolkent, ChemistrySelect **3**(45), 12805 (2018).

[31] İ. Özçeşmeci, M. Özçeşmeci, A. Gül, E. Hamuryudan, Synth. Met. **222**, 344 (2016).

[32] E. Ö. Garip, M. Özçeşmeci, I. Nar, İ. Özçeşmeci, E. Hamuryudan, J. Porphyr. Phthalocyanines **22**(01n03), 198 (2018).

[33] M. Özçeşmeci, E. Özkan, E. Hamuryudan, J. Porphyr. Phthalocyanines **17**(10), 972 (2013).

[34] N. S. Bayliss, J. Chem. Phys. **18**(3), 292 (1950).

[35] W.-F. Law, R. C. W. Liu, J. Jiang, D. K. P. Ng, Inorganica Chim. Acta **256**(1), 147 (1997).

[36] M. Haghighi, F. Tajabadi, S. M. Mahdavi, R. Mohammadpour, N. Taghavinia, Thin Solid Films **669**, 269 (2019).

[37] H. Sarigül, İ. Sorar, Marmara Fen Bilim. Derg. **28**(2), 81 (2016).

[38] Z. N. Kayani, Maria, S. Riaz, S. Naseem, Ceram. Int. **46**(1), 381 (2020).

[39] P. Scherrer, Nachrichten Ges. Wiss. Gött. Math.-Phys. Klasse **1918**, 98 (1918).

[40] H. S. Peiser, Acta Crystallogr. **8**(6), 366 (1955).

[41] A. R. Stokes, A. J. C. Wilson, Proc. Phys. Soc. **56**(3), 174 (1944).

[42] M. Özçeşmeci, I. Sorar, I. Özçeşmeci, E. Hamuryudan, J. Coord. Chem. **71**(15), 2281 (2018).

[43] J. Tauc, Amorphous and Liquid Semiconductors, Tauc J. (eds.), Springer, Boston, MA, 159 (1974).

---

*Corresponding author: sorar@mku.edu.tr